Available online at www.sciencedirect.com
ScienceDirect
Quaternary Research 70 (2008) 240–250
QUATERNARY RESEARCH
www.elsevier.com/locate/yqres

Late Holocene high resolution palaeoclimatic reconstruction inferred from Sebkha Mhabeul, southeast Tunisia

L. Marquer [a,e,*], S. Pomel [b], A. Abichou [c], E. Schulz [d], D. Kaniewski [e], E. Van Campo [e]

[a] *Département de Préhistoire, Muséum National d'Histoire Naturelle, UMR-CNRS 5198, France*
[b] *Laboratoire Environnement Tropical, Equipe DYMSET, Université de Bordeaux 3, UMR-CNRS 5185, France*
[c] *Department of Geography, University of Tunis, Tunisia*
[d] *Geographisches Institüt Am Hubland, Würzburg Universiteit, Germany*
[e] *ECOLAB — Laboratoire d'Ecologie Fonctionnelle, Université de Toulouse, UMR-CNRS-UPS-INPT 5245, France*

Received 25 October 2007
Available online 24 July 2008

Abstract

Relations between climate change and landscape evolution during the last two millennia in southeastern coastal Tunisia have been documented using high-resolution reconstruction of flood history and fire activity in the Sebkha Mhabeul core. The age model, based on tephrochronology, indicates that the core extends from Roman to modern times and encompasses the well-defined climatic periods of the last two millennia. This record provides a first palaeoecological/palaeoclimatic high resolution reconstruction in North Africa using a cross-disciplinary approach with both physical (grey-scale intensity, quartz particles) and biological (charcoal and pollen) indicators. The flood history shows four wet/dry cycles (ca. AD 550–950, 950–1300, 1300–1570 and 1570–1870) of different duration. Major hydrological instabilities are concentrated during the Medieval Climate Anomalies and the early Little Ice Age, between AD 1000 and 1550. Direct correlation between climate and fire cannot be established suggesting that the fire history of the Sebkha environment is mainly influenced by human activity. This study demonstrates the great value of sebkhas as palaeoenvironmental archives.

Keywords: Fire; Climatic changes; Human impact; Late Holocene; Sebkha; Southeast Tunisia

Introduction

There has been a long-standing interest in the study of late Quaternary landscape dynamics in the Mediterranean basin, as this region is very sensitive to climate change and has witnessed strong human influence through polyculture, intensive grazing and deliberate use of fire since millennia (Butzer, 2005). However, available pollen records from North Africa were focused on the last 30,000 yr, and late Holocene palaeoecological data are still scarce (Faust et al., 2004). They are concentrated in Tunisia (Ben Tiba and Reille, 1982; Brun, 1983; Damblon and Vanden Berghen, 1993), Algeria (Salamani, 1993) and Morocco (Reille, 1977; Ballouche and Damblon, 1988; Lamb et al., 1995; Cheddadi et al., 1998). Only one pollen sequence from the Moroccan Atlantic coastline has incorporated a charcoal analysis as a first evidence of the past-fire activity (Damblon, 1991).

Microscopic charcoal has been commonly used to reconstruct the long-term dynamics of fire in the Mediterranean basin at a regional scale (Carrión et al., 2007). In North Africa, the history of human activity, long-term fire dynamics and climate change are closely related (Reale and Dirmeyer, 2000), and it is difficult to disentangle the effects of climate and anthropogenic disturbance on the origins of fire. Climate proxies such as $\delta^{18}O$ and tree-rings, which respond primarily to climatic changes, have provided a first framework of regional climate change study during the late Holocene (Till and Guiot, 1990; Jones et al., 2006). Other proxies, such as grey-scale intensity (Rodbell et al., 1999), grain-size distribution and influx of quartz particles (Lim et al., 2005; Sun et al., 2006), have been used as proxy indicators of climate. We here investigate the reliability

* Corresponding author. Département de Préhistoire, Muséum National d'Histoire Naturelle, 1 rue René Panhard, 75013 Paris (France). Fax: +33 1 43 31 22 79.
E-mail address: marquer@mnhn.fr (L. Marquer).

0033-5894/$ - see front matter © 2008 University of Washington. All rights reserved.
doi:10.1016/j.yqres.2008.06.002

of paleoclimatic inferences from these proxies, particularly as evidence of flood events. A grey scale with quartz and charcoal data from the Sebkha Mabheul (Tunisia) provides a high-temporal resolution history of the hydrological changes, anthropogenic impact and burning activities since AD 250 (1700 cal yr BP). The 75-cm-long core is supported by a chronology based on tephra layers and is used to interpret environmental conditions that prevailed in the southeast coastal Tunisia during the last two millennia, a period of well-known climatic variability.

Environmental setting

North African coastal zones are characterised by the presence of periodically flooded salt depressions, termed sebkhas. The 4-km^2 Sebkha Mhabeul (33°24.58′N, 10°51.01′E, 1 m a.s.l.) is located on the northern edge of the coastal Djeffara plain (Fig. 1). This 40-km-wide plain is covered with marine and lacustrine Quaternary deposits and bordered to the south by an escarpment of Mesozoic limestones (Stengele and Smykatz-Kloss, 1995). The sebkha is disjointed from the eastern larger Sebkha Melah by an accumulation of upper Pleistocene sediments, which avoids any connection of the former to the sea. Its sedimentation mode is mainly controlled by precipitation and runoff from a small wadi system (Schulz et al., 1995, 2002).

The climate is arid Mediterranean type (200–350 mm yr^{-1}) with winter precipitation and a long summer drought. The nearest weather station of Zarzis (33°30.14′N, 11°6.45′E, 5 m a.s.l.) indicates a mean annual precipitation of 225 mm for the period AD 1909–1994. The sebkha is located north of the Saharan complex (Fig. 1), between the 400- and 100-mm isohyets (Le Houérou, 2001). The Mediterranean sclerophyllous forests with *Pinus halepensis*, *Quercus ilex*, *Quercus coccifera*, and shrubs (especially *Pistacia*, *Rosmarinus* and *Phillyrea*) are developed above the 400-mm isohyet. The 100-mm isohyet is the biological limit between steppe and desert. The ecological groups of the steppe are characterized by Poaceae (*Stipa tenacissima*, *Lygeum spartum*), *Artemisia* spp., and Chenopodiaceae. The majority of these landscapes are secondary steppes developed under human pressure (Le Houérou, 1969). The present surrounding vegetation of the sebkha is a semi-desert, where *Olea* plantations are abundant.

Materials and methods

Lithology and mineralogy

A 75-cm-long core was collected in 1993 in the central part of the Sebkha (33°25.02′N, 10°50.52′E, 2 m a.s.l.), using a Kullenberg corer. The retrieved sediments correspond mainly to

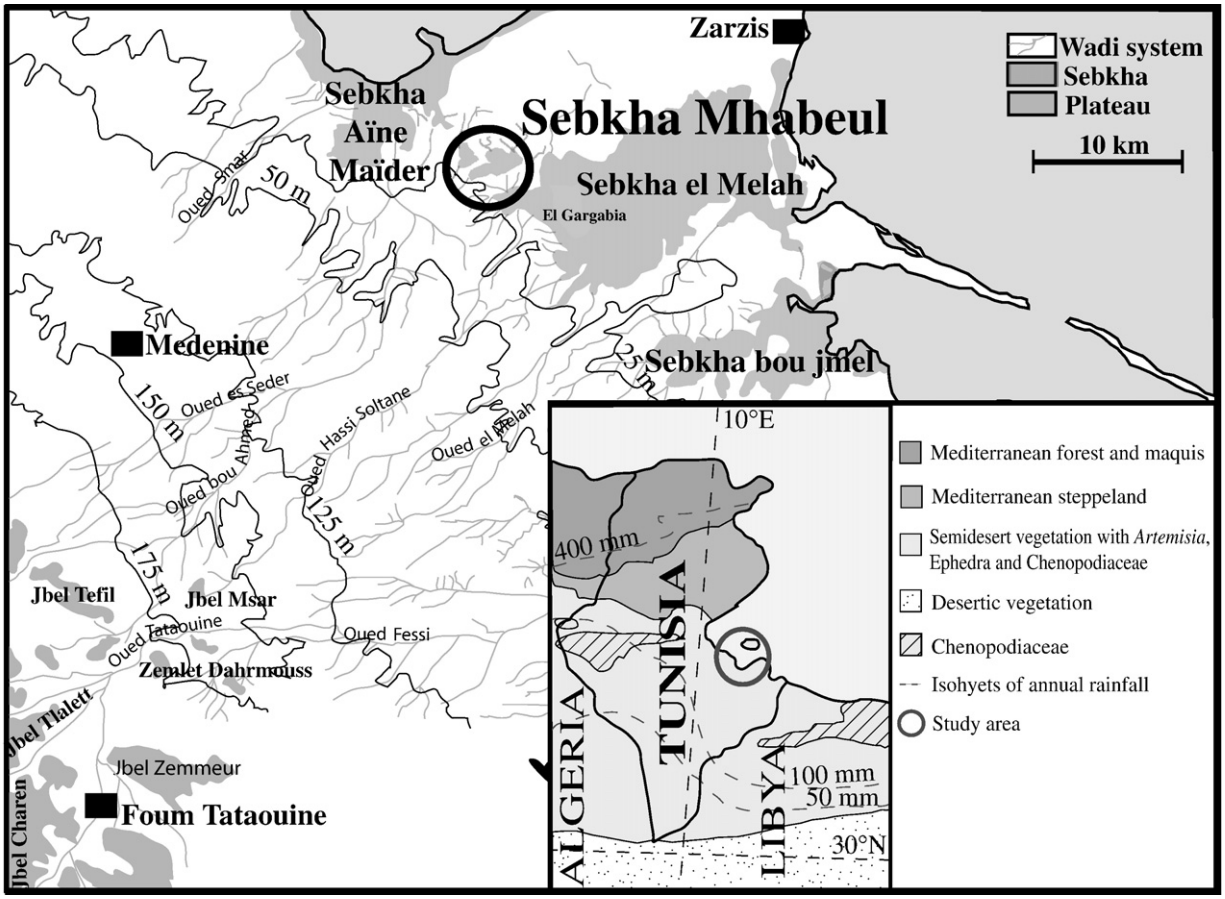

Figure 1. Location of Sebkha Mhabeul in southeast Tunisia; vegetation belts and isohyets are indicated.

https://doi.org/10.1016/j.yqres.2008.06.002 Published online by Cambridge University Press

laminated deposits (Fig. 2). Three ca. 3-cm-thick levels of silty sand are interstratified in the core at 12–15 cm, 40–43 cm and 64–66 cm. The formation of the lamination system in the sebkha has been described by Schulz et al. (2002):

0–1 cm: salt crust
1–6 cm: organic threefold or twofold laminates
6–12 cm: threefold or twofold laminates
12–15 cm: silty sand layer
15–40 cm: threefold or twofold laminates
40–43 cm: silty sand layer
43–64 cm: threefold or twofold laminates
64–66 cm: silty sand layer
From 66 cm to the bottom: threefold or twofold laminates

The laminates are formed after each flooding and are normally threefold. The basic layer consists of light-coloured fine grained detritic material, mainly quartz. Grain-size distribution, morphology and surface texture of the quartz particles have been investigated. Morphoscopy analyses have revealed a dominance of water transport by surface runoff, although potential aeolian contributions cannot be excluded. An

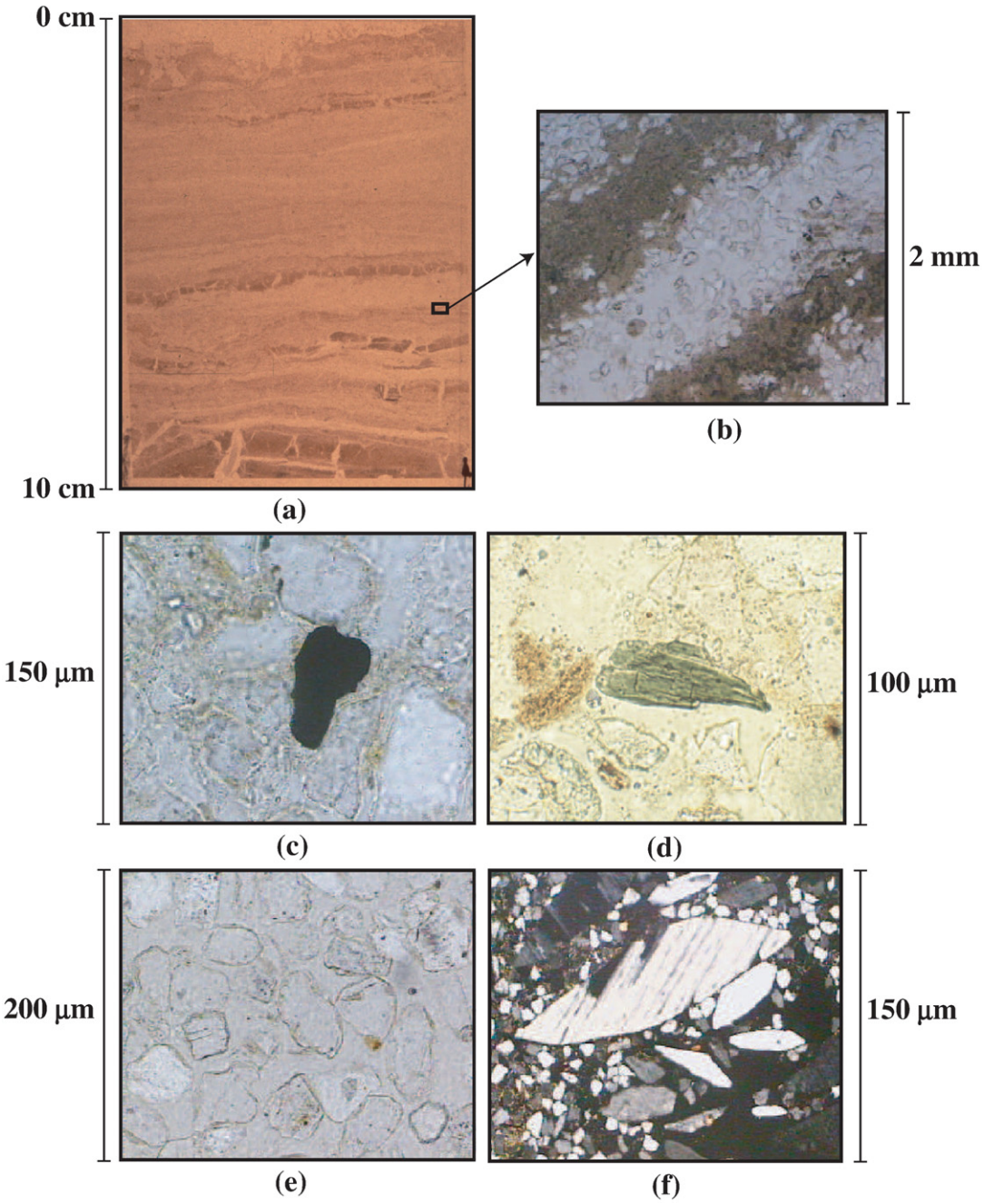

Figure 2. (a) Thin section sediments with laminates, (b) detritic (clear) and cyano-bacterial layers (dark), (c) microscopic charcoal fragment, (d) Tephra (Vesuvius, AD 1631), (e) quartz particles, (f) gypsum particles in polarized light.

https://doi.org/10.1016/j.yqres.2008.06.002 Published online by Cambridge University Press

overlying layer of dark-coloured algae and bacteria mats forms under the water film during the decantation phase. An upper layer of evaporites, either halite or gypsum, terminates the threefold laminates.

A twofold system exists with only a cyanobacterial layer covered by evaporites, mostly gypsum and anhydrite. This latter system forms at the edge of the sebkha, or during periods of minor flooding. It can even form without flooding, with sufficient humidity from dew. Observations on the recent functioning of sebkha in Tunisia have shown that thick evaporitic layers can result from intense wet/dry cycles: large amounts of salts are mobilized during vast inundation periods, and further deposited as thick evaporites during subsequent periods of high insolation. Such cycles are not necessarily annual.

Following this model, clear/dark aspects of the sediment were taken as a proxy for the nature and intensity of flooding events. Downcore, grey-level variability of the sedimentary core was evaluated, using an image analysis technique. An arbitrary scale was established. Maximum grey-scale values are associated with light-coloured evaporitic levels formed during high magnitude flood events followed by total desiccation of the sebkha. This could characterize periods with high frequency of intense precipitation events, most probably during the warm season (late spring to late summer), since subsequent strong surface heating is necessary to induce evaporation. Also, increased water transport capacity resulting from strong runoff events is associated with increased and/or large clear detritic quartz particles. Minimum grey-scale values are associated with dark-coloured intervals, formed during periods of more stable climatic conditions, marked by flood events of lower magnitude or lower frequency.

A Cichorioideae/Chenopodiaceae ratio has been computed to evaluate the impact of the desiccation phase on the pollen preservation in the sebkha during high evaporation phases that might affect the surrounding vegetation. The use of the Cichorioideae as a indicator of differential conservation is well-known in non-littoral arid environments (Bottema, 1975). The Chenopodiaceae are commonly used as an indicator of arid climatic and/or edaphic conditions. This ratio is used to discriminate between the pressure of dry/saline conditions on vegetation (increase of Chenopodiaceae) (Neumann et al., 2007) and the state of conservation directly linked to pollen taphonomy in the sediments (increase of Cichorioideae).

Chronology

The chronology of the core was based on tephrochronology. Eight tephra-layers were detected in the core. Five of them were attributed to eruptions from the Tyrrhenian Sea and three have been precisely dated (Table 1). The AD 79, 1631 and 1930 tephra dates show an orderly relationship with depth and are considered reliable. As no hiatus has been detected in the core, the bulk density corrected deposition rates have been calculated between adjacent tephra layers. They were assumed constant between each age control point and the age of each sample was estimated by interpolation to create an age–depth model (Fig. 3). According to the tephrochronology, the Sebkha Mabheul core covers the last 1700 yr. This time interval encompasses the classically-named Roman Warming Period (RWP) (Reale and Dirmeyer, 2000), the Dark Ages (DA) (Desprat et al., 2003), the Medieval Climate Anomalies (MCA) (Bradley et al., 2003), the Little Ice Age (LIA) (Wiles et al., 2008), and the warming present. The complexity of climate change during this period has been recently emphasized (Jones and Mann, 2004).

Table 1
Tephrochronological study of Sebkha Mhabeul sediments

Depth (cm)	Identified material	Origin	Chronology
1,5	olivine-diopside	Stromboli	AD 1930
9	Augite-diopside	Vesuvius	December 17, AD 1631
73	Augite-diopside and aegyrine augite	Vesuvius	October 24-26, AD 79

Microscopic charcoal

Several methods are used to sample and quantify the microcharcoal fragments (MCFs) from terrestrial and lacustrine sediments (Patterson et al., 1987; Rhodes, 1998). The pollen-slide method is commonly applied (Asselin and Payette, 2005; Davis and Stevenson, 2007) due to an easy count of MCFs and pollen grains from the same slide. As extraction techniques used for pollen preparation can bias the area and number of charcoal particles by breaking the largest pieces (Carcaillet et al., 2001), MCFs have been studied on petrographic thin sections. This method is based on direct observation of charcoal particles within the sediment giving potentially a seasonal reconstruction of fire signals in annually-laminated sediments (Clark, 1988). Twelve continuous thin sections have been prepared from the top of the core down to 66 cm, in order to reconstruct the long-term fire dynamics in the sebkha wide environment.

MCFs have been identified from other dark particles (pyrite and unburned oxidized plant remains), using optical densities and morphological attributes (black, opaque and angular shapes) (Patterson et al., 1987; Clark, 1988). An image analysis method for automated counting of MCFs was applied, using a transmitted light microscope, a video camera and two software suites. MCFs were first visually identified on ten microscopic fields (Fig. 2) selected randomly every 1cm on each thin section. An image of each field was captured using Adobe 4.2.1.L. software and converted to grey levels using Optilab Pro-F.2.6.2 software. The grey levels corresponding to previously identify MCFs were chosen. Two successive anamorphous treatments allowed selecting only charcoal particles on the field. MCFs quantification was made on this last image. The total area and number of fragments were estimated for each field. The results were expressed in mean particle size (μm^2) every 1 cm along the sedimentary core and in area per cm^2 of sediment ($mm^2\ cm^{-2}$), which was converted in microscopic charcoal influx ($mm^2\ cm^{-2}\ yr^{-1}$). MCF size is controlled by several factors including burned plant species, combustion,

https://doi.org/10.1016/j.yqres.2008.06.002 Published online by Cambridge University Press

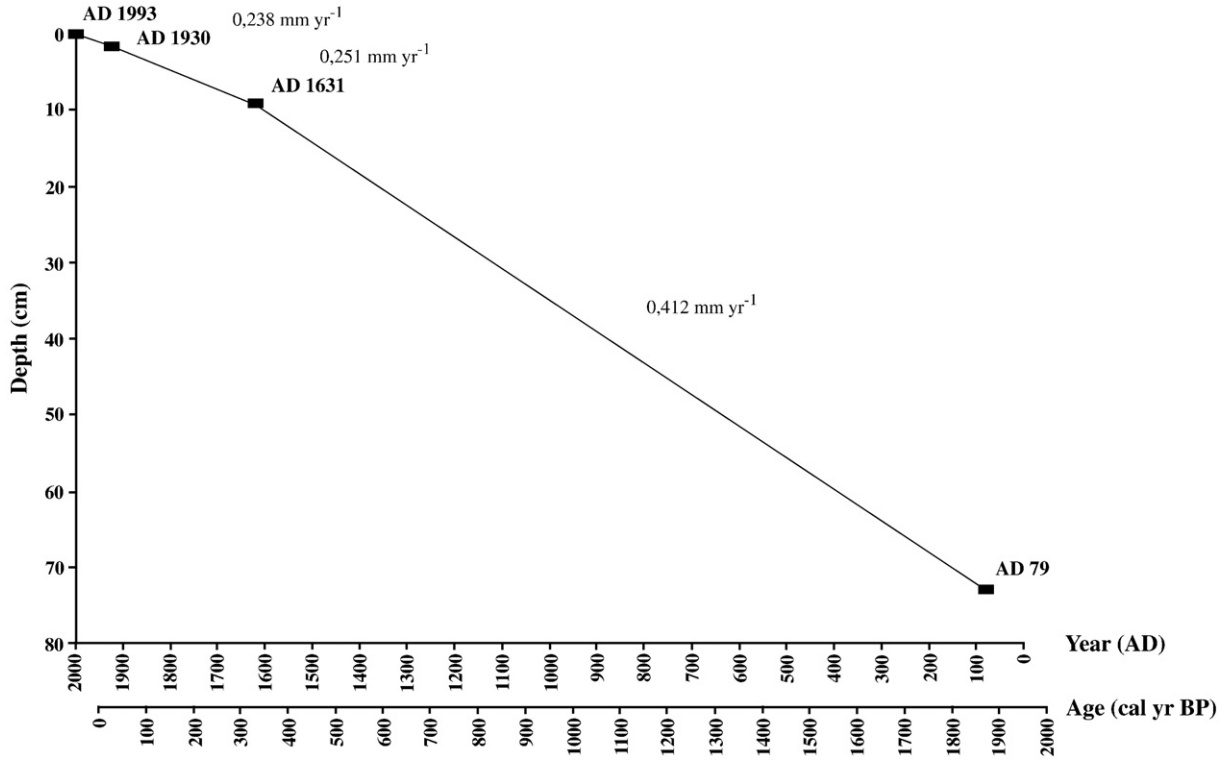

Figure 3. Age–depth model.

dispersion and deposit processes. MCFs are rapidly dispersed, primarily through wind transport during the fire and secondarily, by fluvial transport. The largest fragments are assumed not to have been transported far from fires (Pederson et al., 2005) whereas the smallest fragments can be easily carried by the wind or surface runoff over long distances (Clark, 1988).

Quartz particles

The previous method was adapted to count quartz particles in petrographic thin sections. Quartz particles are siliceous material of detritic origin. They were visually identified on five microscopic fields (Fig. 2) selected randomly every 1 cm on each thin section. An image of each field was captured. The results were expressed in mean particle size (μm^2) every 1 cm along the sedimentary core and in area per cm^2 of sediment (mm^2 cm^{-2}), which were converted in quartz particle influx (mm^2 cm^{-2} yr^{-1}). The size of quartz particles is related to changes in the energy of the hydrological system. Largest particles are indicative of a high-energetic system with a strong competence of surface runoff while smallest particles are transported by a low-energy system or even by wind (Sun et al., 2006). Variations in quartz influx can result from changes in hydrological system induced by floods but also from changes in wind transport, such as during dust storms. From the image analysis, the surface structure of the smallest quartz particles did not allow clear differentiation of water and/or aeolian inputs due to post-depositional erosion processes. The oscillations of the influx is quite complex, with a mixed signal corresponding to both aeolian and water transport.

Results

Grey-scale variability and quartz particles

Grey-scale (GS) intensity shows substantial fluctuations along the core (Fig. 4). These fluctuations, associated with variations in the influx and mean size of quartz particles, document changes in the timing, nature and intensity of flooding events in the sebkha. The evaporation phases, deduced from the grey scale data, are always followed by a peak in the Ci/Ch ratio, which confirms the existence of a changing sedimentary environment and differential conservation processes. The Ci/Ch ratio peaks lag each highest grey-scale peak by ca. 20–30 yr.

The core encompasses the so-called RWP, DA, MCA, LIA and present climate period. Examination of centennial trends in GS intensity reveals large colour shifts around ca. AD 550, 950, 1300, 1550 and 1870. These shifts separate light and dark time intervals lasting several decades to centuries, and indicate major changes in the hydrological functioning of the sebkha. These changes correspond to four complete wet/dry cycles (C1 to C4), whose timing roughly matches the temporal limits of the five distinct conventional climate periods. Each cycle includes major flood events (FE) of differing intensity and duration (Fig. 4).

Until ca. AD 550, during the late RWP, low GS values associated with dark sediments suggest stable climatic

https://doi.org/10.1016/j.yqres.2008.06.002 Published online by Cambridge University Press

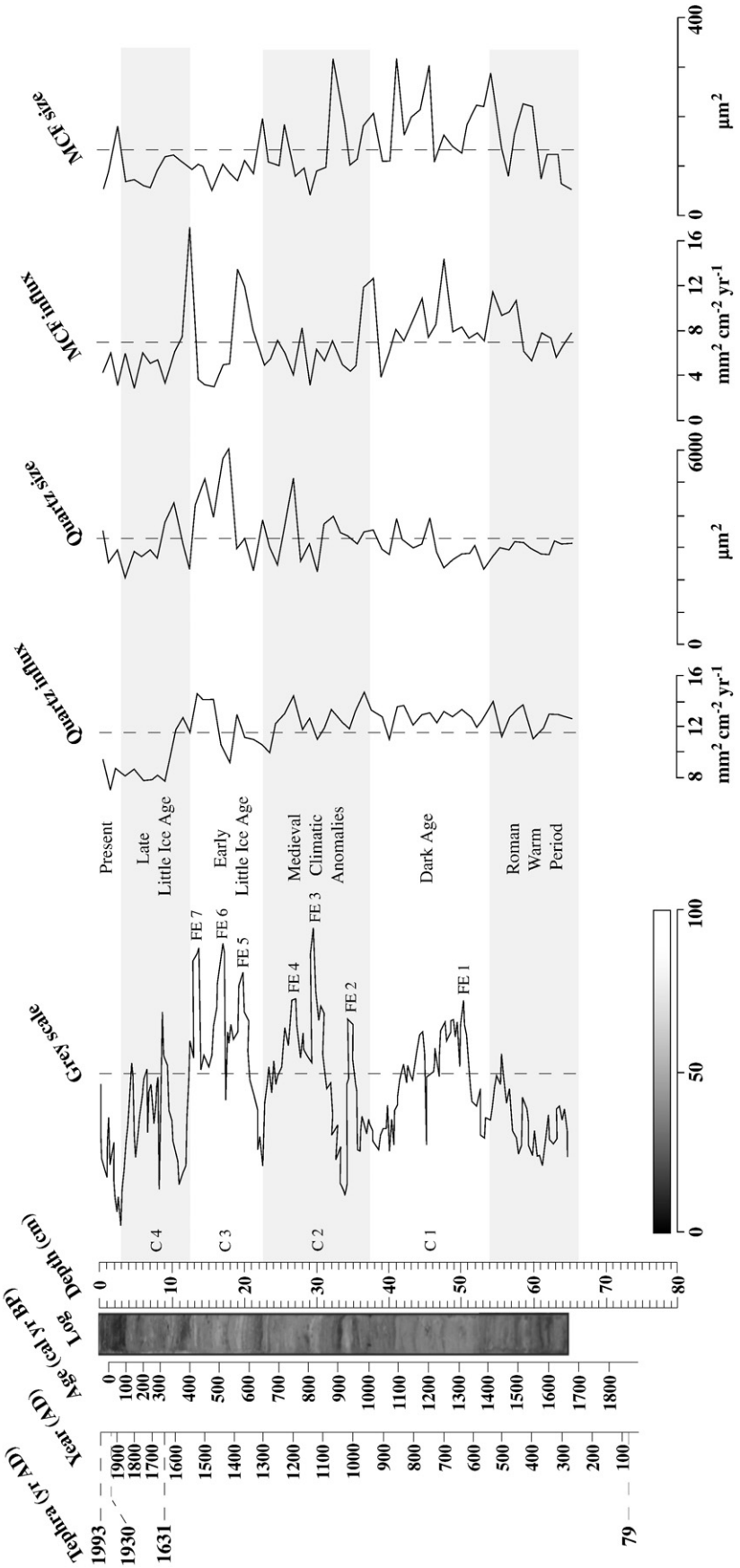

Figure 4. Variations of the grey-scale intensity, and of quartz and microscopic charcoal fragments influx and size. Complete wet/dry climatic cycles are labelled C1 to C4. The first incomplete cycle is not labelled. Major flood events are labelled FE1 to FE7.

https://doi.org/10.1016/j.yqres.2008.06.002 Published online by Cambridge University Press

conditions with small and/or scarce flood events. No major variations are recorded in the quartz influx, and mean particle size remains around the average value.

A first 400-yr cycle from light to dark sediments (C1) is recorded between ca. AD 550 and 950, during the DA. More intense flood events inferred from the dark/light colour shift were suddenly initiated after ca. AD 530. High GS values are registered from ca. AD 590 to 750, suggesting a 160-yr duration for this major flood event FE1. Quartz influx did not record strong variations. A slight drop in the mean size distribution, however, indicates moderate water transport capacity during this interval. A drop in the GS values after ca. AD 750 is interpreted as a return to more stable climatic conditions with small and/or scarce flood events during the following two centuries, in spite of a synchronous slight increase in the mean size of quartz particles.

The initiation of the second cycle C2 is marked by the sharp increase in the GS values, revealing a return to an intense flood activity after ca. AD 950, during the MCA, with three major flood events (FE2, FE3 and FE4). After a short reversal recorded by a sharp decline in the GS values at ca. AD 1000, the highest GS values of the profile around ca. AD 1110–1120 (FE3) suggests that the highest magnitude flood event occurred at that time. The overall decline in the GS values afterwards reflects a progressive return to more stable conditions. Two increases are observed in the mean size particles at ca. AD 935–965 and ca. AD 1070–1100 and an isolated peak at ca. AD 1200.

The GS signal shows a rapid return to high values from ca. AD 1350 to 1540 during cycle C3, corresponding to the early LIA. Intervals of highly positive values indicating 10- to 20-yr episodes of high magnitude flood events ca. AD 1360 (FE5), 1430 (FE6) and 1520 (FE7) alternated with prolonged multi-decadal intervals of intermediate values. In spite of the saw-tooth pattern of the GS curve, the early LIA is characterised by a higher than average GS values. Quartz influx decreases slightly after ca. AD 1350, before reaching the highest value of the series at ca. AD 1520, whereas particle size also registers the major peaks of the series between ca. AD 1410 and 1500, both suggesting an increased water transport capacity. The drop in GS values after ca. AD 1540 marks the end of this contrasted period.

The decrease in the GS values after AD 1520 is followed by a 200-yr interval of higher values, from ca. AD 1650 to 1850. However, the evidence of more quiescent hydrological conditions during the cycle C4 (the late LIA) is supported by intermediate GS values and by a sharp decrease in the quartz influx which reaches the lowest values of the whole series near ca. AD 1850 and is paralleled by a drop in mean particle size which also reaches minimum values at that time.

In the uppermost part of the profile, the establishment of modern conditions is characterised by the return to more unstable conditions after ca. AD 1870.

Micro-charcoal fragments

Abundance and mean size of MCFs are key indicators of wide-area past fire activity. The presence of MCFs in all levels (Fig. 4) suggests a continuous occurrence of burning activities in the sebkha. The existence of heavy rainfall episodes was not sufficient to prevent fires.

The end of the RWP is characterised by low influx of MCF and by small particle sizes; Both increase after ca. AD 450 and size values reach a first maximum near ca. AD 530 (287 μm^2).

During the DA, the average influx of MCFs is higher with significant peaks at ca. AD 700 and 770. The size-values are significantly higher than the average of the whole series. Three high peaks are recorded near ca. AD 750, 855 and 930.

During the MCA and early LIA, the influx of MCFs gradually drops to low values while one isolated peak occurred from ca. AD 1360 to 1390. The size of the MCFs also decrease with only one major peak at ca. AD 1060 (313 μm^2) and two minor peaks at ca. AD 1250 and 1330.

The onset of the late LIA is marked by a last peak in MCF influx at ca. AD 1550 while the rest of this period shows decreases in the MCF influx and mean size which reach lowest values during this period, whereas a slight reversal is observed in both parameters after ca. AD 1850.

Discussion

Changes in the GS intensity, quartz particle sizes, MCFs and pollen (Schulz et al., 2002) in Sebkha Mhabeul provide the first high-resolution environmental history for the last two millennia in this region. The sedimentary deposits of the Sebkha Mabeul can be paralleled to the Holocene sequences of the Sabkha Boujmel, which constitutes the largest evaporitic appendix of Bahira el Bibane (Lakhdar et al., 2006).

Grey-scale, quartz particles and short-term climatic events

From ca. AD 250 to 430, the record is marked by a lack of strong episodes of inundation or dust storms, suggesting stable climatic conditions during the RWP, with a strong increase in the arid/saline Chenopodiaceae pollen type, indicating local arid conditions (Fig. 5). Similar trends have been observed in Italy where flood events of the Tiber River were infrequent compared to the ca. 200 BC–AD 174 period, which suggests a tendency towards drier conditions (Reale and Dirmeyer, 2000). High values in $\delta^{18}O$ record from Nar Gölü-Turkey (Jones et al., 2006) and low precipitation amounts in Lake Gölhisar (Turkey) (Eastwood et al., 2007) are recorded from AD 0 to 500, suggesting a global drought in both the western and eastern Mediterranean basin. A progressive increase in temperature is also specified during this time period (Desprat et al., 2003; Lebreiro et al., 2006). Two arid episodes have been recorded in Lake Tigalmammine (Morocco) (Cheddadi et al., 1998) and correspond with decreased $\Delta^{14}C$ values (Stuiver et al., 1998), suggesting a high solar irradiance.

From ca. AD 430 onwards, a progressive increase in flood event intensity and/or frequency was observed with a local increase in aquatic plants starting since ca. AD 530. Higher water-discharge, suggesting the first shift to unstable climatic conditions (C1), occurred after AD 550. This cycle includes the first major flood event FE1, with two minor positive oscillations at ca. AD

https://doi.org/10.1016/j.yqres.2008.06.002 Published online by Cambridge University Press

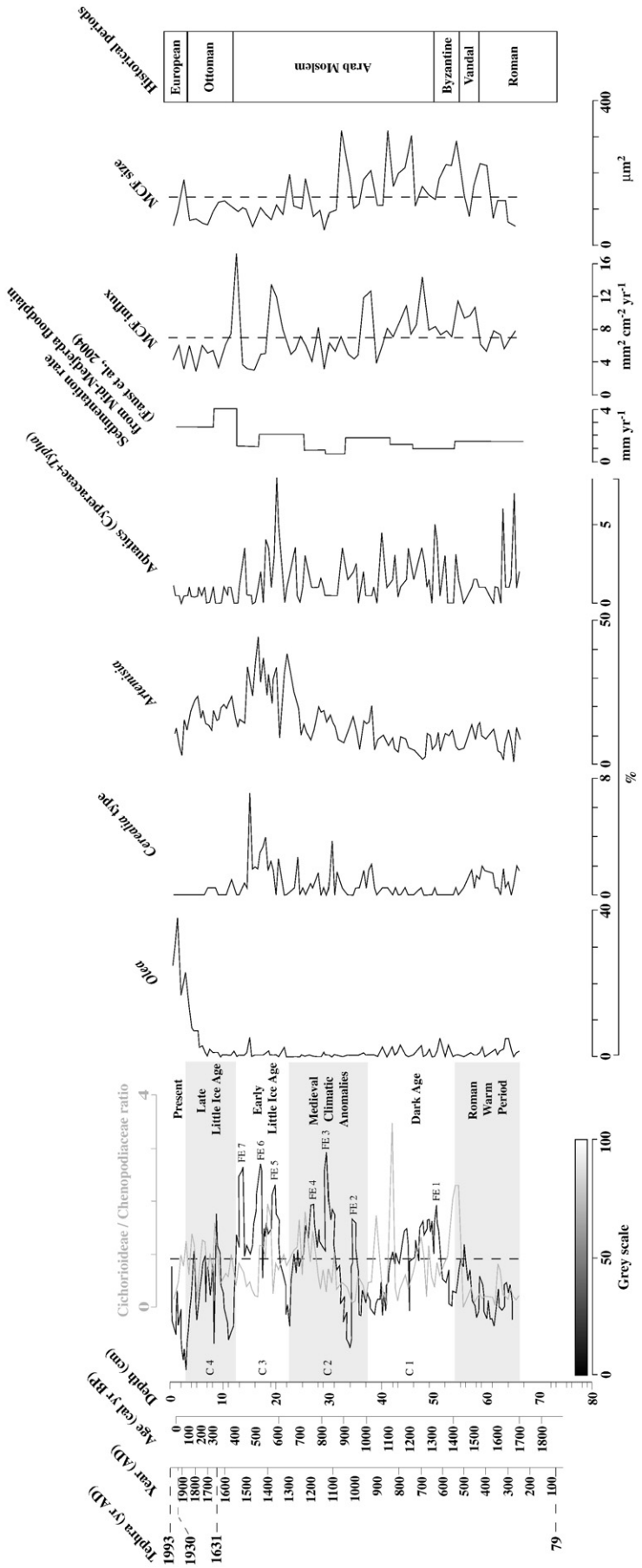

Figure 5. Synthesis of the Sebkha environmental history since AD 250. Complete wet/dry climatic cycles are labelled C1 to C4. The first incomplete cycle is not labelled. Major flood events are labelled FE1 to FE7.

https://doi.org/10.1016/j.yqres.2008.06.002 Published online by Cambridge University Press

590 and 750. In the Medjerda floodplain of northern Tunisia (Faust et al., 2004), heavy flooding appears since ca. AD 500; in the Tiber River (Italy) after the 5th century AD, dry and wet phases alternated with heavy flood events (Reale and Dirmeyer, 2000). Important climatic changes led to a fall in temperature (Mann and Jones, 2003), a decrease of solar activity (Stuiver et al., 1998) and the development of wetter conditions (Jones et al., 2006; Magny et al., 2007). In the eastern Mediterranean Sea, strong decreases in $\delta^{18}O$ indicate a maximum precipitation at ca. AD 700 (Schilman et al., 2001) followed by a trend towards higher values, suggesting drier conditions between AD 900 and 1100. A similar trend towards drier conditions is recorded in the sebkha during the second part of the DA (ca. AD 750–950). This time period corresponds with a return to more stable climatic conditions during two centuries, with a regular precipitation pattern. In the Nar Gölü isotope sequence, a positive shift in $\delta^{18}O$ centred around AD 900 indicates lower precipitation and/or higher evaporation (Jones et al., 2006).

From ca. AD 950 to 1300, during cycle C2, short-term periods of intense inundation events FE2, FE3, and FE4 are recorded in the Sebkha Mhabeul. The hydrological anomalies are characterized in the sebkha core by a higher input of large particles that suggest two ca. 30-yr heavy rainfall episodes before (ca. AD 935–965) and after (ca. AD 1070–1100) the Oort Minimum (AD 1010–1050), a period of enhanced fluvial dynamics in northern Tunisia (Faust et al., 2004). In the Nar Gölü isotope sequence, more negative $\delta^{18}O$ values indicative of higher precipitation/lower evaporation occurred during this time period, with several oscillations of the $\delta^{18}O$ curve suggesting strong variability within this interval. An important flood event occurs at ca. AD 1200, correlated with less saline conditions in Lac Ichkeul (northern Tunisia) (Stevenson et al., 1993). Around AD 1280–1305, more stable conditions at Sebkha Mabeul characterized the Wolf Minimum (AD 1280–1340). Widespread climatic anomalies have been previously defined the Medieval Climatic Anomaly (MCA) (Bradley et al., 2003) or Medieval Warm Period (MWP) (Keller, 2004). This period includes a phase of increased solar irradiance, of high levels of explosive volcanism and of hydrological anomalies centred on the Grand Solar Maximum (AD 1100–1250) (Zicheng and Ito, 2000) which led to prolonged drought and exceptional rains (Till and Guiot, 1990; Bradley et al., 2003).

The onset of the Little Ice Age (LIA; AD 1400 to 1850) (Stuiver et al., 1997; Bradley et al., 2003) corresponds in the Sebkha Mhabeul with the three major ca. 10–30 yr episodes of heavy rainfall and inundation phases FE5, FE6 and FE7 during cycle C3. The ca. AD 1420–1430 and ca. AD 1510–1525 episodes are included in the Spörer minimum (AD 1420–1530) while the last one (ca. AD 1640–1645) is correlated with disastrous flood events in the mid-Medjerda basin (Faust et al., 2004). A centennial increase in precipitation has been recorded in lake Gölhisar around ca. AD 1500 followed by a sharp drop in the annual amount (Eastwood et al., 2007). All these events have occurred in the Sebkha Mhabeul environment before the Maunder minimum (AD 1645–1715). After ca. AD 1645, the intermediate climatic state, which characterizes cycle C4, marks the late LIA with a progressive trend towards more regular hydrological conditions without pronounced inundation events. A reversal trend was initiated after ca. AD 1870.

The grey-scale and quartz particle records from the Sebkha Mabeul core appear to be climate-sensitive and fit well with the main climatic periods defined for the last two millennia in the Mediterranean basin. Previous studies from the near Sabkha Boujmel have suggested that the sediments of the uppermost part of the Holocene were laid down under a dry climate (Lakhdar et al., 2006). The Sebkha Mabeul record has detailed this time period and suggests that a succession of short-term climatic events (floods or heavy rainfalls) has occurred in the area during the last 1700 yr.

Fire activities and short-term climatic events

Fire activities cover the wide environment of the Sebkha and can be driven by climate and/or human factors. Comparison between the fire remains and the climatically controlled GS and quartz records helps to discriminate between a natural or anthropogenic origin of fires.

The mean size distributions of MCF and of quartz particles (Fig. 4) show an opposite evolution during the last two millennia suggesting different causal processes. The higher sizes of MCF are concentrated from the end of the RWP to the onset of the MCA. Since ca. AD 1100, the mean size values sharply drop until modern times.

High influx of MCFs corresponds to large fires (Mensing et al., 1999) but can also relate to increased water and/or wind-transport of charcoal particles following a burning event (Pederson et al., 2005). In this arid and salty area, important changes in water discharge likely played a role in the increase of MCF size and influx. Climate, however, was probably not the main trigger for fire, as with the strong anthropogenic impact in North Tunisia during the last millennia.

Fire activity and human pressures

The pollen record of Sebkha Mabeul (Schulz et al., 1995, 2002) reveals the human pressure on the regional landscape since at least Roman times (Fig. 5), which is well-documented for the western Mediterranean basin (Reale and Dirmeyer, 2000). During the Roman period, fire activities are low while pollen types indicative of polyculture, with cereal cultivation and arboriculture (mainly *Olea europaea*), are recorded (Schulz et al., 1995, 2002). These data suggest that slash-and-burn agriculture was not intensively used for economical purpose during this period.

An important fire activity is recorded between ca. AD 450 and 1100. Several peaks of MCF mean sizes at ca. AD 400–430, 530, 745, 850 and 1070 suggest strong fire events during the unstable socio-economic phase corresponding with the Vandal conquest after Carthage's fall in AD 439. The Vandal period ended in AD 533 with the onset of the Byzantine era and the following Arab conquest at AD 647 (Fig. 5). These periods were marked by several wars and consequent changes on agro-pastoral activities, which might explain an increased fire activity.

https://doi.org/10.1016/j.yqres.2008.06.002 Published online by Cambridge University Press

During the last millennium, fire events decreased during the Arab-Muslim and Ottoman eras. The intensity of fire signals is low since ca. AD 1100, while the greatest changes are observed in all proxies (*Artemisia*, *Cerealia* type, quartz particle influx and size) during the medieval time. These data suggest an abandonment of slash-and-burn activities as a component of agro-pastoral practices and a stable socio-economic system without wars. Brun (1983) suggests that this period corresponds to a sedentary phase on the coastal zone marked by the development of cereals and olive orchards. The existence of inland nomad zones is suggested by the spread of a pasture-induced *Artemisia* steppes. Fire events at ca. AD 1230 and 1300 might be inferred to these pastoral activities. At the end of the Arab-Muslim era, the data show a low fire activity that slightly increases again with the European presence in Tunisia.

Fire activity in the Sebkha Mhabeul area was probably under human control, as the MCF oscillations appear to be linked to the historical events in northern Africa. No clear correlation emerges between fires and the flood history.

Conclusion

The great interest of sebkhas as palaeoenvironmental archives, suggested by Schulz et al. (2002) and Lakhdar et al. (2006), is confirmed by the multi-proxy (grey scale, quartz particles, micro-charcoal fragments and pollen) study of the laminated sediments from the Sebkha Mhabeul. This record provides the first palaeoecological and palaeoclimatic high-resolution reconstruction (average 8 yr between two samples) for the last 1700 yr, with both physical and biological indicators giving a cross-disciplinary approach of the links between landscape and climate.

Short-term climatic events (floods or heavy rainfalls) recorded in the sedimentary filling fit with four wet/dry cycles, roughly corresponding with classical climatic periods previously identified in the Mediterranean basin. The major hydrological instabilities are concentrated during the Medieval Climate Anomalies and the early Little Ice Age.

The fire history of the Sebkha environment seems clearly influenced by changes in regional economy and wars from ca. AD 430 to 1100, although direct correlation between climate and fire cannot be established. As this study concerns a single core, natural fire cannot be definitively excluded and additional analyses are required to state the real influence of climatic changes as a potential trigger of fire in the coastal zone.

Acknowledgments

We are indebted to the Deutsche Forschungsgemeinschaft, the Ecole Supérieure d'Horticulture Chott Mariem and PICS franco-allemands OPS n° 521 of CNRS for financial and technical support. We wish to thank Dr. Mohamed Soussi and an anonymous reviewer for valuable suggestions, as well as Thierry Otto, Jean-Jacques Dedoubat and Nicolas Skuli for technical help.

References

Asselin, H., Payette, S., 2005. Detecting local-scale fire episodes on pollen slides. Review of Palaeobotany and Palynology 137, 31–40.

Ballouche, A., Damblon, F., 1988. Nouvelles données palynologiques sur la végétation holocène du Maroc. Institut français de Pondichéry 25, 83–90.

Ben Tiba, B., Reille, M., 1982. Recherches pollenanalytiques dans les montagnes de Kroumirie (Tunisie septentrionale): premiers résultat. Ecologia Mediterranea 8 (4), 75–86.

Bottema, S., 1975. The interpretation of pollen spectra from prehistoric settlements (with special attention to Liguliflorae). Palaeohistoria 17, 18–35.

Bradley, R.S., Hughes, M.K., Diaz, H.F., 2003. Climate in Medieval Time. Science 302, 404–405.

Brun, A., 1983. Etude palynologique des sédiments marins holocènes de 5000 BP à l'actuel dans le golfe de Gabès (mer pélagienne). Pollen et Spores XXV 3–4, 437–460.

Butzer, K.W., 2005. Environmental history in the Mediterranean world: cross-disciplinary investigation of cause-and-effect for degradation and soil erosion. Journal of Archaeological Science 32, 1773–1800.

Carcaillet, C., Bouvier, M., Fréchette, B., Larouche, A.C., Richard, P.J.H., 2001. Comparison of pollen-slide and sieving methods in lacustrine charcoal analyses for local and regional fire history. The Holocene 11 (4), 467–476.

Carrion, J.S., Fuentes, N., Gonzales-Samperiz, P., Sanchez Quirante, L., Finlayson, J.C., Fernandez, S., Andrade, A., 2007. Holocene environmental change in a montane region of southern Europe with a long history of human settlement. Quaternary Science Reviews 26, 1455–1475.

Cheddadi, R., Lamb, H.F., Giot, J., Van Der Kaars, S., 1998. Holocene climatic change in Morocco: a quantitative reconstruction from pollen data. Climate Dynamics 14, 883–890.

Clark, J.S., 1988. Stratigraphic charcoal analysis on petrographic thin sections : application to fire history in northwestern Minnesota. Quaternary Research 30, 81–91.

Damblon, F., 1991. Contribution pollenanalytique à l'histoire des forêts de chêne liège au Maroc: La subéraie de Krimda. Palaeoecology of Africa 22, 171–190.

Damblon, F., Vanden Berghen, C., 1993. Etude paléo-écologique (pollen et macrorestes) d'un dépôt tourbeux dans l'île de Djerba, Tunisie méridionale. Palynosciences 2, 157–172.

Davis, B.A.S., Stevenson, A.C., 2007. The 8.2ka event and Early? Mid Holocene forests, fires and flooding in the Central Ebro Desert, NE Spain. Quaternary Science Reviews 26, 1695–1712.

Desprat, S., Sanchez Goni, M.F., Loutre, M.-F., 2003. Revealing climatic variability of the last three millennia in northwestern Iberia using pollen influx data. Earth and Planetary Science Letters 213, 63–78.

Eastwood, W.J., Leng, M.J., Roberts, N., Davis, B., 2007. Holocene climate change in the eastern Mediterranean region: a comparison of stable isotope and pollen data from Lake Gölhisar, southwest Turkey. Journal of Quaternary Science 22 (4), 327–341.

Faust, D., Zielhofer, C., Baena Escudero, R., Diaz del Olmo, F., 2004. High-resolution fluvial record of late Holocene geomorphic change in northern Tunisia: climatic or human impact? Quaternary Science Reviews 23, 1757–1775.

Jones, P.D., Mann, M.E., 2004. Climate over past millennia. Reviews of Geophysics 42, 1–42.

Jones, M.D., Roberts, N., Leng, M.J., Türkes, M., 2006. A high-resolution late Holocene lake isotope record from Turkey and links to North Atlantic and monsoon climate. Geology 34 (5), 361–364.

Keller, C.F., 2004. 1000 years of climate change. Advances in Space Research 34, 315–322.

Lamb, H.F., Gasse, F., Benkadour, A., El Hamouti, N., Van Der Kaars, S., Perkins, W.T., Pearce, N.J., Roberts, N., 1995. Relation between century-scale Holocene arid intervals in tropical and temperate zones. Nature 373, 134–137.

Lakhdar, R., Soussi, M., Ben Ismail, M.H., M'Rabet, A., 2006. A Mediterranean Holocene restricted coastal laggon under arid climate: case of the sedimentary record of the Sabkha Boujmel (SE Tunisia). Palaeogeography, Palaeoclimatology, Palaeoecology 241, 177–191.

Lebreiro, S.M., Frances, G., Abrantes, F.F.G., Diz, P., Bartels-Jonsdottir, H.B., Stroynowski, Z.N., Gil, I.M., Pena, L.D., Rodrigues, T., Jones, P.D., Nombela, M.A., Alejo, I., Briffa, K.R., Harris, I., Grimalt, J.O., 2006. Climate change and coastal hydrographic response along the Atlantic Iberian margin (Tagus Prodelta and Muros Ria) during the last two millennia. The Holocene 16 (7), 1003–1015.

Le Houérou, H.N., 1969. La végétation de la Tunisie Steppique. Annales de l'institut national de la recherche agronomique de Tunisie 42 624 p.

Le Houérou, H.N., 2001. Biogeography of the arid steppeland north of the Sahara. Journal of Arid Environments 48, 103–128.

Lim, J., Matsumoto, E., Kitagawa, H., 2005. Eolian quartz flux variations in Cheju Island, Korea, during the last 6500 yr and a possible Sun-monsoon linkage. Quaternary Research 64, 12–20.

Magny, M., de Beaulieu, J.L., Drecher-Schneider, R., Vannière, B., Walter-Simonnet, A.V., Miras, Y., Millet, L., Bossuet, G., Peyron, O., Brugiapaglia, E., Leroux, A., 2007. Holocene climate changes in the central Mediterranean as recorded by lake-level fluctuations at Lake Accesa (Tuscany, Italy). Quaternary Science Reviews 26, 1736–1758.

Mann, M.E., Jones, P.D., 2003. Global surface temperatures over the past two millennia. Geophysical Research Letters 30, 51–54.

Mensing, S.A., Michaelsen, J., Byrne, R., 1999. A 560-year record of Santa Ana fires reconstructed from charcoal deposited in the Santa Barbara Basin, California. Quaternary Research 51 (3), 295–305.

Neumann, F.H., Kagan, E.J., Schwab, M.J., Stein, M., 2007. Palynology, sedimentology and palaeoecology of the late Holocene Dead Sea. Quaternary Science Reviews 26 (11–12), 1476–1498.

Patterson, W.A., Edwards, K.J., Maguire, D.J., 1987. Microscopic charcoal as a fossil indicator of fire. Quaternary Science Reviews 6, 3–23.

Pederson, D.C., Peteet, D.M., Kurdyla, D., Guilderson, T., 2005. Medieval Warming, Little Ice Age, and European impact on the environment during the last millennium in the lower Hudson Valley, New York, USA. Quaternary Research 63, 238–249.

Reale, O., Dirmeyer, P., 2000. Modeling the effects of vegetation on Mediterranean climate during the Roman Classical Period. Part I: Climate history and model sensitivity. Global and Planetary Change 25, 163–184.

Reille, M., 1977. Contribution pollenanalytique à l'histoire holocène de la végétation des montagnes du Rif (Maroc Septentrional). Recherches françaises sur le Quaternaire, supplément au Bulletin de l'AFEQ 1 (50), 53–76.

Rhodes, A.N., 1998. A method for the preparation and quantification of microscopic charcoal from terrestrial and lacustrine sediment cores. The Holocene 8 (1), 113–117.

Rodbell, D.T., Seltzer, G.O., Anderson, D.M., Abbott, M.B., Enfield, D.B., Newman, J.H., 1999. An 15,000-year record of El Nino-driven alluviation in southwestern Ecuador. Science 283, 516–520.

Salamani, M., 1993. Premières données paléophytogéographiques du cèdre de l'Atlas (*Cedrus atlantica*) dans la région de Grande Kabylie (NE Algérie). Palynosciences 2, 147–155.

Schilman, B., Bar-Matthews, M., Almogi-Labin, A., Luz, B., 2001. Global climate instability reflected by Eastern Mediterranean marine records during the late Holocene. Palaeogeography, Palaeoclimatology, Palaeoecology 176, 157–176.

Schulz, E., Smykatz-Kloss, W., Abichou, H., Fromm, R., Pomel, S., Salzmann, U., Sponholz, B., Stengele, F., Ben Tiba, B., Hachicha, T., 1995. Zaderg environmental history of the semidesert region in southern Tunisia. Geologisches Zentralblatt, Paläont. Teil I (3–4), 423–440.

Schulz, E., Abichou, A., Hachicha, T., Pomel, S., Salzmann, U., Zouari, K., 2002. Sebkhas as ecological archives and the vegetation and landscape history of southern Tunisia during the last two millennia. Journal of African Earth Sciences 34, 223–229.

Sun, Y., Lu, H., An, Z., 2006. Grain size of loess, palaeosol and red clay deposits on the Chinese Loess Plateau : significance for understanding pedogenic alteration and palaeomonsoon evolution. Palaeogeography, Palaeoclimatology, Palaeoecology 241, 129–138.

Stengele, F., Smykatz-Kloss, W., 1995. Mineralogical and geochemical study of holocene sebkha sediments in Southeastern Tunisia. Chemide Erde 55, 241–256.

Stevenson, A.C., Phethean, S.J., Robinson, J.E., 1993. The palaeosalinity and vegetational history of Garaet el Ichkeul, northwest Tunisia. The Holocene 3, 201–210.

Stuiver, M., Braziunas, T.F., Grootes, P.M., Zielinski, G.A., 1997. Is there evidence for solar forcing of climate in the GISP2 oxygen isotope record? Quaternary Research 48, 259–266.

Stuiver, M., Reimer, P.J., Bard, E., Beck, J.W., Bur, G.S., Hughen, K.A., Kromer, B., McConrad, G., Van der Plicht, J., Spurk, M., 1998. INTCAL98 radiocarbon age calibration, 24,000–0 cal BP. Radiocarbon 40, 1041–1083.

Till, C., Guiot, J., 1990. Reconstruction of precipitation in Morocco since 1100 AD based on *Cerus atlantica* tree-ring widths. Quaternary Research 33, 337–351.

Wiles, G.C., Barclay, D.J., Calkin, P.E., Lowell, T.V., 2008. Century to millennial-scale temperature variations for the last two thousand years indicated from glacial geologic records of Southern Alaska. Global and Planetary Change 60, 115–125.

Zicheng, Y., Ito, E., 2000. Historical solar variability and mid-continent drought. Pages Newsl. 8, 6–7.